Chromatographia (2011) 74:215–226
DOI 10.1007/s10337-011-2068-5

ORIGINAL

Analysis of 2-Amino-1-methyl-6-phenylimidazo[4,5-*b*]pyridine and Its Phase I and Phase II Metabolites in Mouse Urine Using LC–UV–MS–MS

S. F. Teunissen · H. Rosing · L. Brunsveld · T. F. A. de Greef · S. Durmus · J. H. M. Schellens · A. H. Schinkel · J. H. Beijnen

Received: 11 March 2011 / Revised: 1 May 2011 / Accepted: 9 May 2011 / Published online: 24 May 2011

Abstract 2-Amino-1-methyl-6-phenylimidazo[4,5-*b*]pyridine (PhIP) is an abundantly present heterocyclic aromatic amine which is found to be carcinogenic in rodents, mice and rats. The biotransformation of PhIP is extensive and involves both the formation of bioactivated as well as detoxification metabolites. In order to understand its carcinogenicity, the metabolism of PhIP needs to be studied. Numerous metabolites of PhIP have been described but, so far, assays for their quantitative determination in biological matrices are scarce. We present the development and application of an assay, using reversed phase liquid chromatography coupled to ultraviolet and mass spectrometry detectors for the quantification of PhIP, three phase I and nine phase II metabolites in urine. Additionally, the identification of two PhIP-sulfates by the use of NMR is presented. Sample pretreatment consisted of straightforward dilution of urine. PhIP and its metabolites were shown to be stable in diluted urine for at least 22 h when stored at 2–8 °C. Precision of the analysis was within 15%. The assay has been successfully applied for the quantification of PhIP and 12 of its metabolites in urine from mice that received 200 mg kg^{-1} PhIP via oral gavage.

Keywords HPLC–UV–MS–MS, PhIP · Metabolites · Urine

Electronic supplementary material The online version of this article (doi:10.1007/s10337-011-2068-5) contains supplementary material, which is available to authorized users.

S. F. Teunissen (✉) · H. Rosing · J. H. Beijnen
Department of Pharmacy and Pharmacology,
Slotervaart Hospital/The Netherlands Cancer Institute,
Louwesweg 6, 1066 EC Amsterdam, The Netherlands
e-mail: Bas.Teunissen@slz.nl

L. Brunsveld · T. F. A. de Greef
Laboratory of Chemical Biology, Department of Biomedical Engineering, Eindhoven University of Technology,
Den Dolech 2, 5612 AZ Eindhoven, The Netherlands

S. Durmus · A. H. Schinkel
Division of Molecular Biology,
The Netherlands Cancer Institute, Plesmanlaan 121,
1066 CX Amsterdam, The Netherlands

J. H. M. Schellens
Department of Clinical Pharmacology,
The Netherlands Cancer Institute, Plesmanlaan 121,
1066 CX Amsterdam, The Netherlands

J. H. M. Schellens · J. H. Beijnen
Department of Pharmaceutical Sciences, Faculty of Science,
Utrecht University, 3508 TB Utrecht, The Netherlands

Introduction

2-Amino-1-methyl-6-phenylimidazo[4,5-*b*]pyridine (PhIP) is one of the most abundant heterocyclic aromatic amines (HAAs). HAAs are a class of carcinogenic compounds found in proteinaceous foods such as cooked meats and fish [1]. PhIP is formed from phenylalanine, creatinine and glucose as a by-product of the Maillard reaction during cooking or frying of protein-rich foods at high temperatures [2, 3]. It is a carcinogenic compound in rodents and induces lymphomas, mammary carcinomas and colon and prostate carcinomas in mice, female rats and male rats, respectively [4–8].

The metabolism of PhIP is extensive. Its activation and detoxification depends on the formation of various metabolites. Bioactivation is believed to proceed via *N*-hydroxylation (Table 1; R_2) at the amine group by CYP1A1 and CYP1A2 [9–14]. This results in the formation of 2-hydroxyamino-1-methyl-6-phenylimidazo[4,5-*b*]pyridine (N2-OH-PhIP). N2-acetoxy-PhIP and N2-sulfonyloxy-PhIP

Table 1 Trivial names, chemical structures and molecular masses of PhIP and its metabolites

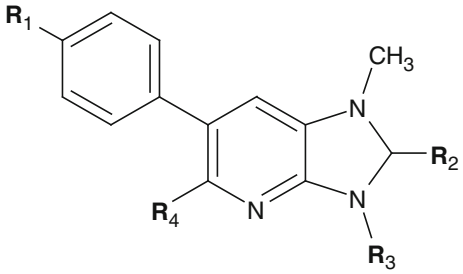

Trivial name	Analyte number	R_1	R_2	R_3	R_4	Formula	Mol. Mass
PhIP	1	H	NH_2	–	H	$C_{13}H_{12}N_4$	224.1
N2-methyl-PhIP	2	H	NH–CH3	–	H	$C_{14}H_{14}N_4$	238.1
N2-OH-PhIP	3	H	NH–OH	–	H	$C_{13}H_{12}N_4O$	240.1
5-OH-PhIP	4	H	NH2	–	OH	$C_{13}H_{12}N_4O$	240.1
PhIP-4′-sulfate	5	Sulfate	NH2	–	H	$C_{13}H_{12}N_4O_4S$	320.1
PhIP-5-sulfate	6	H	NH2	–	Sulfate	$C_{13}H_{12}N_4O_4S$	320.1
N2,4′-diOH-PhIP-sulfate	7	Sulfate	NH2	–	OH	$C_{13}H_{12}N_4O_5S$	336.1
PhIP-N3-glucuronide	8	H	=NH	Gluc	H	$C_{19}H_{20}N_4O_6$	400.1
PhIP-N2-glucuronide	9	H	NH–gluc	–	H	$C_{19}H_{20}N_4O_6$	400.1
4′-OH-PhIP-glucuronide	10,11,12 or 13	O-Gluc	NH2	–	H	$C_{19}H_{20}N_4O_7$	416.1
5-OH-PhIP-glucuronide	10,11,12 or 13	H	NH2	–	O-Gluc	$C_{19}H_{20}N_4O_7$	416.1
4′-OH-PhIP-N2-glucuronide	10,11,12 or 13	OH	NH–gluc	–	H	$C_{19}H_{20}N_4O_7$	416.1
N2-OH-PhIP-N2-glucuronide	10,11,12 or 13	H	N(OH)–gluc	–	H	$C_{19}H_{20}N_4O_7$	416.1
N2-OH-PhIP-N3-glucuronide	10,11,12 or 13	H	=N–OH	Gluc	H	$C_{19}H_{20}N_4O_7$	416.1

The molecular mass is based on the monoisotopic mass. '=' is used to indicate the presence of a double bond between the amine and the imidazole moiety. If R_3 is: '–', a C=N double bond is present between the 2 and 3 position of the imidazole moiety

Gluc glucuronide, *PhIP* 2-amino-1-methyl-6-phenylimidazo[4,5-*b*]pyridine, R_1 4′-position; R_2 N2-position; R_3 N3-position

are subsequently formed from N2-OH-PhIP by acetyltransferases [15–17] and sulfotransferases [15, 17–20], respectively. These phase II metabolites are unstable and the sulfate and acetate group is cleaved off heterolytically under formation of nitrenes and/or nitrenium ions which can form adducts with DNA purines [21–23]. The instability of both metabolites might be the reason why they have not been recovered from any matrix hitherto. After binding of PhIP to DNA purines, a product is formed via a thus far unknown pathway. This product/metabolite, 5-OH-PhIP, is believed to be a marker for mutagenesis [24–26]. Like PhIP, N2-OH-PhIP and 4′-OH-PhIP, 5-OH-PhIP can undergo sulfation and glucuronidation, thereby forming detoxified metabolites which are readily excreted [27–31]. Some PhIP phase I and phase II metabolites were first described by Chen et al. [12]. Data on whether these metabolites can be considered detoxified or activated products is lacking and so is data on the extent of formation in vivo. Numerous assays have been developed for the quantification of PhIP in various matrices [32, 33]. However, the number of publications reporting on the quantification of PhIP metabolites is very scarce and includes only minor fractions of currently known PhIP metabolites [24, 30, 34, 35].

Most ideally, analytes are quantified by use of a certified reference standard of each analyte. Calibration standards are then prepared and the response of an analyte is subsequently interpolated on the calibration curve to calculate its concentration. Certified reference standards of metabolites, however, are rarely available which makes their quantification a challenging task. In this case, a different approach is required. We present hereby an assay based on liquid chromatography coupled to ultraviolet and mass spectrometry detection, in which PhIP and both its three phase I and nine phase II metabolites (Table 1) are quantified in mouse urine based on their ultraviolet and mass spectrometry responses. Additionally, the application of the assay is demonstrated by quantification of PhIP and its metabolites in 24 h urine from mice which have received by oral gavage 200 mg PhIP per kg.

Experimental

Chemicals and Reagents

2-Amino-1-methyl-6-phenylimidazo[4,5-*b*]pyridine was purchased from Toronto Research Chemicals (North York,

Table 2 HPLC gradient parameters for LC–UV–MS analysis on two coupled Synergi Polar 80 Å columns (150 × 2.0 mm I.D., 4 μm) at 60 °C

Time (min)	Flow rate (mL min^{-1})	Mobile phase A[a] (%)	Mobile phase B[b] (%)
0.0	0.3	90	10
30.0	0.3	50	50
30.1	0.3	90	10
33.0	0.3	90	10

[a] Mobile phase A 10 mM ammonium acetate pH 7.0

[b] Mobile phase B 100% acetonitrile

Ontario, Canada). 2-Hydroxyamino-1-methyl-6-phenylimidazo[4,5-*b*]pyridine (N2-OH-PhIP) was purchased from the National Cancer Institute Chemical Carcinogen Reference Standard Repository at the Midwest Research Institute (Kansas City, USA). 2-Amino-1-methyl-6-phenylimidazo[4,5-*b*]-5-hydroxypyridine (5-OH-PhIP) was a kind gift from Henrik Frandsen of the National Food Institute, Technical University of Denmark. LiChrosolv water for HPLC and formic acid were from Merck (Darmstadt, Germany). Methanol originated from Biosolve Ltd. (Amsterdam, The Netherlands). Isofluorane was from Teva Pharmachemie (Haarlem, The Netherlands). β-Glucuronidase and all other chemicals and reagents were from Sigma-Aldrich (Steinheim, Germany).

Instrumentation

Liquid Chromatography–Ultraviolet–Mass Spectrometry Detection

High performance liquid chromatography–ultraviolet–mass spectrometry (HPLC–UV–MS) experiments were performed using an Accela chromatography system (Thermo Fisher Scientific, Waltham, MA, USA), consisting of a quaternary solvent delivery system, in-line degasser, autosampler, column oven and a photodiode array detector. Mobile phase A consisted of a 10-mM ammonium acetate solution pH 7.0. Mobile phase B consisted of acetonitrile. Mobile phases A and B were pumped through two connected Synergi Polar 80 Å columns (150 × 2.0 mm I.D., 4 μm; Phenomenex, Torrance, CA, USA) at a flow rate of 0.3 mL min^{-1} using a linear gradient as shown in Table 2. The analytical column was protected by a 4 × 2.0 mm I.D. guard column. The separation was performed at 60 °C. Volumes of 15 μL were injected using an autosampler thermostatted at 7 °C. The total run time was 33 min. The autosampler needle was rinsed with methanol before injection. The LC eluate was directed via the photodiode array detector into an LTQ XL Linear Ion Trap mass spectrometer (Thermo Fisher Scientific) equipped with an electrospray ionization source operating in the positive ion mode. Multiple reaction monitoring (MRM) spectra were acquired with LCquan™ software (Thermo Fisher Scientific). Positive ions were created at atmospheric pressure using an ion spray voltage of 4 kV and sheath, auxiliary and ion sweep gas at 40, 15 and 15 arbitrary units, respectively. The capillary temperature was set at 350 °C. The photodiode array detector was set at either scanning mode for measuring absorption spectra, or at specific wavelengths of 306, 318 and 340 nm, respectively.

Liquid Chromatography–Mass Spectrometry Detection

HPLC–MS experiments were performed on an Agilent 1100 series liquid chromatography system (Agilent technologies, Palo Alto, CA, USA) consisting of a binary pump, an in-line degasser, autosampler and column oven. Mobile phase A was prepared by adjusting a 5-mM ammonium formate solution to pH 3.5 with a 98% formic acid solution. Mobile phase B consisted of methanol. Mobile phases A and B were pumped through a Synergi Hydro 110 Å column (150 × 2.0 mm I.D., 4 μm; Phenomenex, Torrance, CA, USA), at a flow rate of 0.2 mL min^{-1} using a linear gradient as shown in Table 3. The analytical column was protected by a 4 × 2.0 mm I.D. guard column. The separation was performed at 40 °C. Volumes of 15 μL were injected using an autosampler thermostatted at 7 °C. The total run time was 19 min. The autosampler needle was rinsed with methanol before injection. The LC eluate was directed into a Finnigan TSQ Quantum Ultra triple quadrupole mass spectrometer equipped with an electrospray ionization source (Thermo Fisher Scientific) operating in the positive ion mode. For quantification MRM chromatograms were acquired with LCquan™ software. Positive ions were created at atmospheric pressure using an ion spray voltage of 4 kV and sheath, auxiliary and ion sweep gas at 40, 15 and 1.5 arbitrary units, respectively. The capillary temperature was set at 350 °C. The quadrupoles were operating at unit resolution (0.7 Da). During the first 1.5 and last 1.0 min the eluate was directed to waste using a divert valve to prevent the introduction of endogenous compounds into the mass spectrometer.

Table 3 HPLC gradient parameters for LC–MS–MS analysis on a Phenomenex Synergi Hydro 110 Å column (150 × 2.0 mm I.D., 4 μm) at 40 °C

Time (min)	Flow rate (mL min^{-1})	Mobile phase A[a] (%)	Mobile phase B[b] (%)
0.0	0.2	80	20
13.0	0.2	20	80
16.0	0.2	20	80
16.1	0.2	80	20
19.0	0.2	80	20

[a] Mobile phase A 5.0 mM ammonium formate buffer pH 3.5

[b] Mobile phase B 100% methanol

Animals

Mice were housed and handled according to institutional guidelines complying with Dutch legislation. All animals were of >99% FVB background, male and between 8 and 12 weeks of age. Animals were kept in a temperature-controlled environment with a 12-h light/12-h dark cycle. They received a standard diet (AM-II, Hope Farms, Woerden, The Netherlands) and acidified water ad libitum.

Urinary Excretion of PhIP and its Metabolites

A mass balance study was performed with Ruco Type M/1 stainless steel metabolic cages (Valkenswaard, The Netherlands). Male wild-type mice ($n = 5$) of >99% FVB background were allowed to accustom to the cages for 24 h before receiving PhIP (200 mg kg^{-1}) via oral gavage. Urine was collected in a 0–16 h fraction after drug administration. At the end of the experiment, mice were killed by terminal bleeding through cardiac puncture under isofluorane anesthesia, followed by cervical dislocation.

Sample Preparation

After sampling, urine was snap frozen on dry-ice and stored at −70 °C. After thawing, urine was diluted 10× and 100× for UV and MS analysis, respectively. Dilutions were made in a 5 mM ammonium formate buffer pH 3.5. The diluted urine was subsequently transferred to an autosampler vial and stored at 2–8 °C until analysis.

Preparation of PhIP Standard Solutions

Two separate stock solutions of PhIP (1 mg mL^{-1}) were prepared. Approximately, 1 mg was accurately weighed and dissolved in 1 mL methanol. The preparation of the two stock solutions was checked and deviated less than ±5% from each other. One of both stock solutions was used for quantification purposes.

β-Glucuronidase Incubations

β-Glucuronidase from *Escherichia coli* in the form of lyophilized powder was dissolved in a 0.5 M sodium hydrogen phosphate buffer pH 8.0. 1.5 mL of the β-glucuronidase/buffer mixture and 8.5 mL water were added to 20 μL urine. For a blank incubation, 1.5 mL buffer without β-glucuronidase was used. The reaction was performed at 37 °C and terminated after 24 h by adding acetonitrile in a volume of 3:1, subsequent vortex mixing for 15 s and centrifugation for 10 min at 11,300×*g*. The clear supernatant was diluted 1:1 (*v/v*) with 5 mM ammonium formate buffer pH 3.5, vortex mixed for 10 s, subsequently transferred to an autosampler vial and stored at 2–8 °C until analysis.

NMR Identification of Sulfated PhIP metabolites

Urine Preparation for NMR Identification

2-Amino-1-methyl-6-phenylimidazo[4,5-*b*]pyridine was administered to mice (50 mg kg^{-1}) via oral gavage. Urine was collected over a period of 24 h, subsequently freeze-dried and reconstituted in 4 mL methanol–5 mM ammonium formate buffer pH 3.5 (10:90, *v/v*). Reconstituted urine was centrifugated for 5 min at 11,300×*g*. The clear supernatant was subsequently injected onto a Waters 1525 EF LC system. Liquid chromatography was performed on a Waters Atlantis C18 column (250 × 20 mm I.D., 10 μm; Waters Corporation, Milford, MA, USA) using a flow rate of 15 mL min^{-1} and a mixture of 5 mM ammonium formate buffer pH 3.5 (eluent A) and acetonitrile (eluent B) as the mobile phase. Detection was performed using a dual wavelength detector (200 and 254 nm). The compounds were eluted from the column by gradient elution. At time zero a ratio of A–B (90:10, *v/v*) was pumped through the column. A linear gradient was applied from time zero to 60 min to an A–B composition of 60:40 (*v/v*). The liquid eluting from the LC column was collected in 15 mL

fractions. The presence of PhIP metabolites in each fraction was determined using the LC–MS–MS set-up as described above. Two sulfated PhIP metabolites were present in two fractions which we called fraction 1 and 2, respectively. These fractions were freeze-dried and subsequently prepared for NMR analysis by reconstitution in 50 μL of d_6-DMSO.

NMR Identification

All NMR data were recorded on a 500 MHZ NMR (Varian Unity Inova, Agilent technologies, Palo Alto, CA, USA) by means of a Varian indirect-detection HX nanoprobe equipped with pulsed field gradients with the sample spun at 3.5 kHz. The isolated metabolite samples which were dissolved in 50 μL of d_6-DMSO were transferred via a 100 μL Hamilton syringe to the nanoprobe cell. The temperature was actively controlled at 298 K (PhIP and fraction 2) or 323 K (fraction 1). For all measurements the 90° ^{1}H pulse width was calibrated. All spectra were referenced to internal tetramethylsilane (TMS).

Gradient selective HMQC experiments were performed using a relaxation delay time of 2 s, a sweep width of 6,000 Hz for proton dimension and 22,624 Hz for the carbon dimension. All 2D-data were collected in the phase-sensitive mode using the States–Haberkorn method. A total of 512 FIDs of 2K complex data points were collected in t2 with 64 scans per increment. The $^1J_{C-H}$ coupling constant was set to 160 Hz. TANGO gradient suppression was applied to filter residual ^{1}H coupled to ^{12}C. Processing was done after Gaussian apodization in both dimensions. Calibration of the decoupler pulse widths and decoupler strength was achieved using standard calibration procedures.

Gradient enhanced correlation spectroscopy (gCOSY) was performed using a relaxation delay of 2 s and a sweep width of 6,000 Hz. A total of 512 FIDs of 2K complex data points were collected in t2 with 16–32 scans per increment and zero-filling was applied in both dimensions before Fourier transformation. These data were then processed with unshifted cosinebell-squared window function in both dimensions. The DOSY bipolar pulse pair stimulated echo with convection compensation (Dbppste_cc) sequence was used for the determination of the self-diffusion of the different components [36]. In a typical experiment, 64 transients (with a recycle delay of 3 s per transient) for each of the 100 steps were recorded with increasing gradient strength, where gradient pulse duration, diffusion delay and maximum gradient strength were adjusted in order to obtain an 80% reduction of the signal at the highest gradient strength. The experimental diffusion data was obtained using the Stejskal–Tanner equation [37]. (Supplementary data: Online Resource 1-3).

Validation Procedures

Precision and Stability

The inter-assay precision of the LC–UV–MS and LC–MS–MS assay was determined by analysis of a urine sample in fivefold and threefold, respectively. The stability in diluted urine of all metabolites, including PhIP, was demonstrated during storage in an autosampler at 2–8 °C. The precision should not exceed 15%. PhIP and its metabolites are considered stable when the measured concentration is within ±15% of the initial concentration.

Results and Discussion

Chromatography

The LC gradient which was used for LC–MS–MS analysis, was previously developed for the quantification of PhIP and N2-OH-PhIP in various matrices [33].

This gradient was, however, not applicable for LC–UV–MS analysis. When UV detection is used, analytes need to be baseline separated for accurate quantification. A new gradient was therefore developed in which baseline separation was obtained (Fig. 1). The HPLC column from the original method (Synergi Hydro; 150 × 2.0 mm I.D., 4 μm; Phenomenex, Torrance, CA, USA), was unable to provide the necessary resolution at each tested mobile phase composition. Methanol and acetonitrile were tested to serve as organic modifier. An aqueous solution was tested of which the pH was varied from 3.5 to 7.0 using either ammonium formate or ammonium acetate. A Synergi Polar (150 × 2.0 mm I.D., 4 μm; Phenomenex, Torrance, CA, USA), combined with a mobile phase composed of acetonitrile and a 10 mM ammonium acetate solution at pH 7.0 provided nearly the resolution needed for baseline separation of PhIP metabolites and endogenous urine constituents. The analytical column was coupled to an additional Synergi Polar column of the same length. This increase in column length in combination with an increase in temperature to 60 °C provided sufficient resolution for baseline separation of all 13 analytes and endogenous constituents using a long shallow gradient.

Identification of Metabolites

Reference standards, mass spectrometric fragmentation, relative retention time, UV absorbance, degradation by β-glucuronidase, and NMR spectroscopy were used for the identification of PhIP metabolites in mouse urine. Urine recovered from mice which received 200 mg kg^{-1} PhIP p.o., was diluted 10× and injected onto the LC–UV–MS

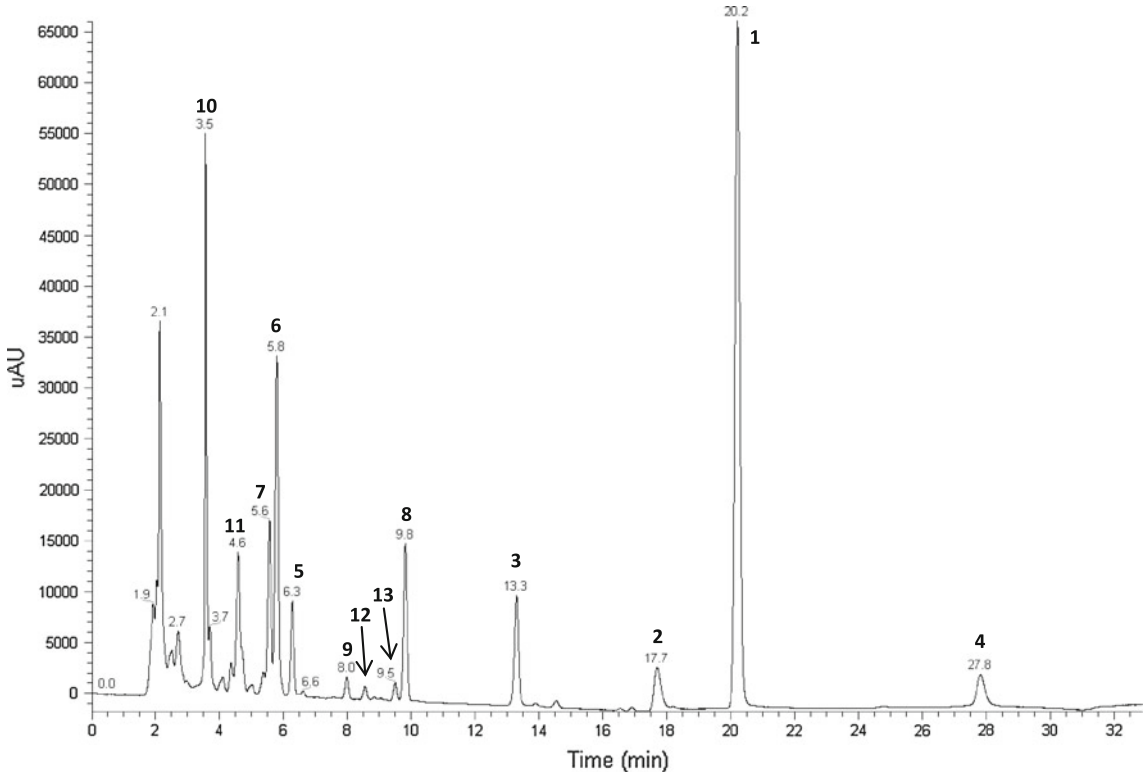

Fig. 1 LC–UV chromatogram of PhIP phase I and II metabolites recovered from urine of a mouse treated with 200 mg kg^{-1} PhIP p.o. Chromatography as described in Table 2. (**1**) PhIP ($t_r = 20.2$ min), (**2**) N2-OH-PhIP ($t_r = 17.7$ min), (**3**) 5-OH-PhIP ($t_r = 13.3$ min), (**4**) N2-methyl-PhIP ($t_r = 27.8$ min), (**5**) PhIP-4′-sulfate ($t_r = 6.3$ min), (**6**) PhIP-5-sulfate ($t_r = 5.8$ min), (**7**) N2,4′-diOH-PhIP-sulfate ($t_r = 5.6$ min), (**8**) PhIP-N2-glucuronide ($t_r = 9.8$ min), (**9**) PhIP-N3-glucuronide ($t_r = 8.0$ min), (**10**) OH-PhIP-glucuronide_1 ($t_r = 3.5$ min), (**11**) OH-PhIP-glucuronide_2 ($t_r = 4.6$ min), (**12**) OH-PhIP-glucuronide_3 ($t_r = 8.5$ min), (**13**) OH-PhIP-glucuronide_4 ($t_r = 9.5$ min)

system. LC eluent was let via a photodiode array UV detector into the linear ion trap mass spectrometer. This allowed for simultaneous UV detection and mass spectrometric identification of compounds eluting from the column.

*(**1**) PhIP, (**2**) N2-OH-PhIP, (**3**) 5-OH-PhIP*

Parental PhIP (225/210 *m/z*), and two of its phase I metabolites: N2-OH-PhIP (241/223 *m/z*) and 5-OH-PhIP (241/223 *m/z*) were unambiguously identified in urine. Their retention time, parent and product mass and UV absorbance spectra were compared with authentic standards and literature [12, 38]. One other known hydroxylated PhIP metabolite, namely 4′-OH-PhIP, was not identified in urine [32].

*(**4**) N2-Methyl-PhIP*

Methylated at the terminal amine (Table 1; R_2), this metabolite is more lipophilic than PhIP. It was observed to elute several minutes after PhIP, in agreement with literature [12]. The fragmentation spectrum of N2-methyl-PhIP (239 *m/z*), with predominant fragments at *m/z* 224, 196 and 179 positively identified this metabolite. UV absorption data of N2-methyl-PhIP has, to the best of our knowledge never been published before. Identification was therefore based on retention time and mass spectrometric fragmentation pattern.

*(**5**) PhIP-4′-sulfate, (**6**) PhIP-5-sulfate*

PhIP-5-sulfate was recently, for the first time, recovered from mice urine by Chen et al. [12]. This metabolite, can be considered a surrogate marker for the formation of the ultimate genotoxic molecule, similar to 5-OH-PhIP [25]. In the contrast, PhIP-4′-sulfate is considered a detoxification metabolite [27, 28]. Both metabolites have equal UV absorption spectra and show minor differences in MS–MS fragmentation spectra which could therefore not be used to distinguish between both metabolites. The large difference in pharmacological properties of both sulfates, however, stresses the importance to distinguish between both metabolites. Therefore, additional to MS–MS and UV absorbance data, NMR spectra were recorded for identification purposes.

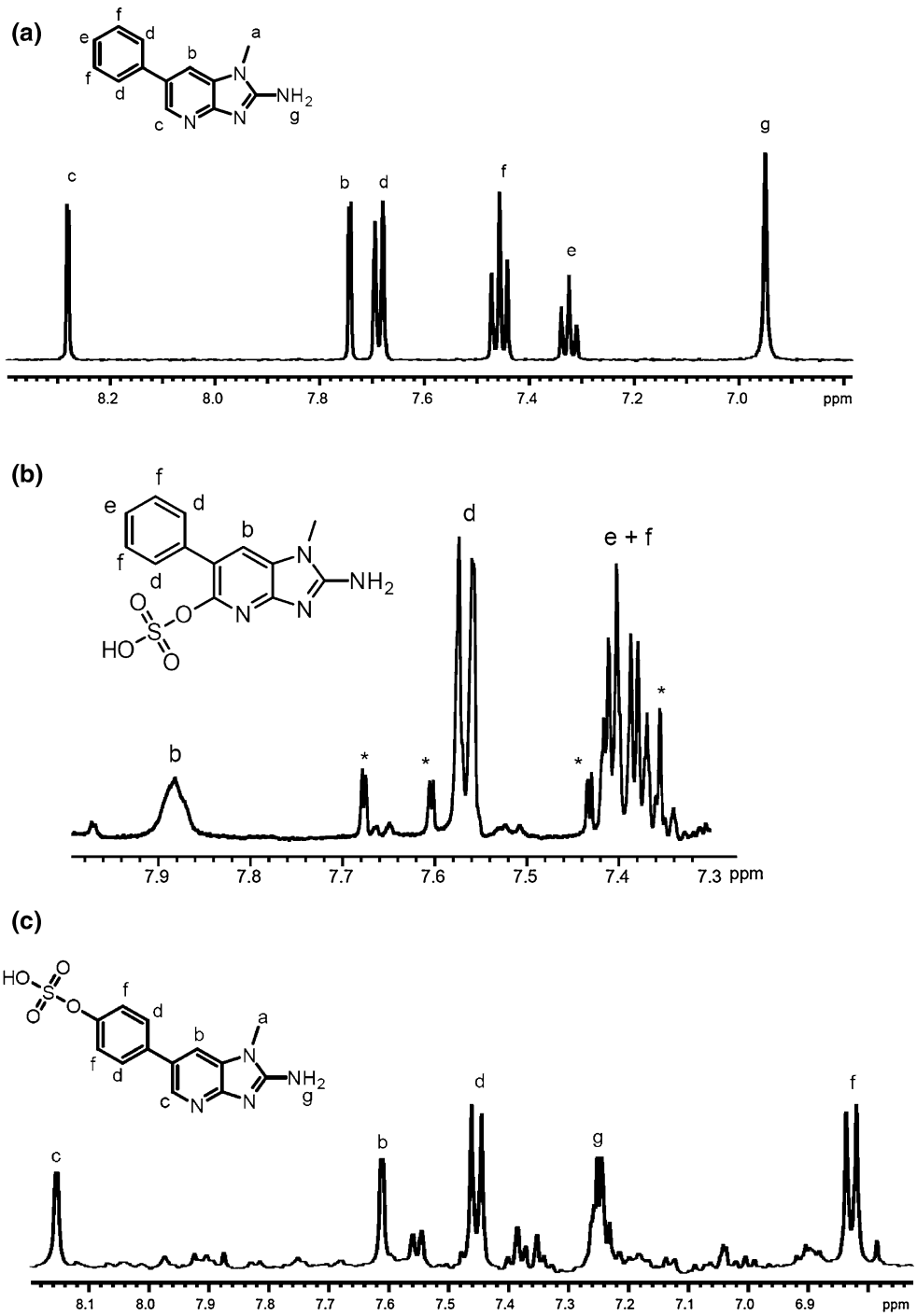

Fig. 2 Recorded NMR spectra of **a** a reference standard of PhIP, **b** fraction 1, in which the NMR spectrum is attributed to the presence of PhIP-5-sulfate, **c** fraction 2, in which the NMR spectrum is attributed to the presence of PhIP-4′-sulfate. *Asterisks* indicates impurity

Two fractions were collected, fraction 1 and fraction 2. Two unidentified sulfated PhIP metabolites were present in fraction 1 and 2, respectively. Fraction 1 and fraction 2, as well as a PhIP reference standard, were analyzed by NMR.

Figure 2a, b show the NMR spectra obtained from a PhIP reference standard and from fraction 1, respectively. The spectrum of fraction 1 (Fig. 2b) clearly shows the disappearance of the characteristic proton at the 5-H position (at ~8.2 ppm in PhIP) which is a very strong indication that a chemical reaction/metabolism step has taken place at the 5-position. Figure 2b additionally shows a shift (compared to Fig. 2a) in signal from protons which are located at position b, d, e and f, which is implicated to be the result from the sulfate group at the 5-position. Figure 2c shows the NMR spectrum obtained from fraction 2. In this spectrum the proton at the 5-H position is still clearly present, in contrast to the spectrum of faction 1. However, the coupling pattern for the phenyl ring has become more simple, resulting in two coupled doublets of equal intensity (twice two protons for d and f). These NMR

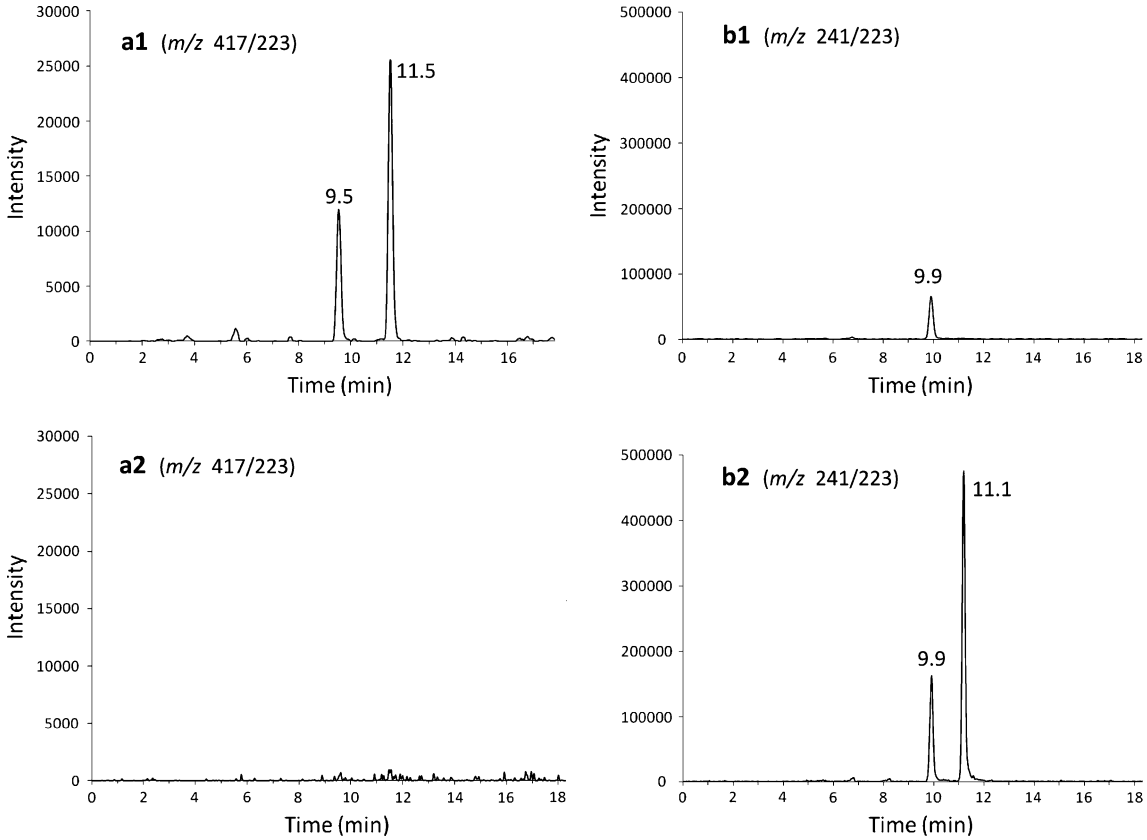

Fig. 3 LC–MS–MS chromatograms of a urinary extract from a mouse treated with 200 mg kg^{-1} PhIP p.o. Chromatography as described in Table 3. **a1**, **a2** response in 417/223 *m/z* window without and with treatment of *β*-glucuronidase, respectively. OH-PhIP-glucuronide_3 (t_r = 9.5 min); OH-PhIP-glucuronide_4 (t_r = 11.5 min). **b1**, **b2** response in 241/223 *m/z* window without and with treatment of *β*-glucuronidase, respectively. 5-OH-PhIP (t_r = 9.9 min), N2-OH-PhIP (t_r = 11.1 min)

data thus clearly point to the addition of a sulfate group at the 4′-position in the metabolite in fraction 2.

The MS–MS spectra of fraction 1 and fraction 2 showed the presence of two compounds with a parent and product mass of 321 and 241 *m/z*, respectively. That data, combined with the above described NMR spectra, confirmed the identity of PhIP-5-sulfate and PhIP-4′-sulfate in fraction 1 and fraction 2, respectively. Both fractions were subsequently analyzed using the LC–UV–MS and LC–MS–MS set-up as described above and the retention time of both sulfates in these fractions was noted. This retention time, combined with the mass transition of both sulfates, was then used for identification purposes in mouse urine.

*(**7**) N2,4′-diOH-PhIP-sulfate*

Two hydroxylated PhIP-sulfate metabolites are known [12]: N2,4′-diOH-PhIP-sulfate and 5,4′-diOH-PhIP-sulfate. We recovered only one hydroxylated PhIP-sulfate from mouse urine. Based on the fact that 5,4′-diOH-PhIP-sulfate is formed in abundance in mice than N2,4′-diOH-PhIP-sulfate, the metabolite that we recovered from mice urine was expected to be 5,4′-diOH-PhIP-sulfate [12]. However, an MS–MS spectrum of N2,4′-diOH-PhIP-sulfate shows a distinct fragment with a mass of 320 *m/z* corresponding with the loss of the terminal hydroxyl group, under formation of PhIP-4′-sulfate (320 *m/z*) [12]. This unique MS–MS fragmentation spectrum positively identified this metabolite as N2,4′-diOH-PhIP-sulfate.

*(**8**) PhIP-N2-glucuronide, (**9**) PhIP-N3-glucuronide*

2-Amino-1-methyl-6-phenylimidazo[4,5-*b*]pyridine is known to have two locations which are preferred for addition of a glucuronide group: the N2, located at the terminal amine, and the N3, located in the imidazole moiety (Table 1) [32]. Both metabolites differ predominantly from each other in terms of UV absorbance and polarity and have a distinct mass transition of 401/225 *m/z* due to the loss of glucuronic acid. The maximum absorption wavelength of PhIP-N2-glucuronide (318 nm) and PhIP-N3-glucuronide (306 nm) was in agreement with literature data [30, 39]. The literature indicates that PhIP-N3-glucuronide is more polar than PhIP-N2-glucuronide

[12, 39, 40]. In combination with the UV absorption data, the PhIP glucuronide eluting first was identified as PhIP-N3-glucuronide (Fig. 1; peak 9) while the second eluting PhIP glucuronide was identified as PhIP-N2-glucuronide (Fig. 1; peak 8).

*(**10–13**) OH-PhIP-glucuronide_1-4*

A combination of hydroxylation and subsequent glucuronidation of PhIP results in five known phase II metabolites [12, 32]. We observed only four of them which might be due to sensitivity constraints. These metabolites, which we named OH-PhIP-glucuronide_1-4 have a parent mass of 417 *m/z* and fragmented all by loss of the glucuronide moiety (176 *m/z*) under formation of hydroxylated PhIP (241 *m/z*). Additionally, OH-PhIP-glucuronide_3 and _4 also fragmented with the simultaneous loss of the glucuronide and hydroxyl moiety under formation of a fragment of 223 *m/z*. Unfortunately, in agreement with the literature, the exact position of both the hydroxyl and glucuronide moiety cannot be unambiguously determined on the basis of the fragmentation spectra. UV absorption data of these metabolite have, to the best of our knowledge never been published before. *β*-glucuronidase incubations supported the hypothesis that these were indeed glucuronidated PhIP metabolites.

β-Glucuronidase Incubations

β-Glucuronidase incubations were used to support the identification of glucuronidated PhIP metabolites. For identification, chromatograms of two samples were compared: (i) a urine sample from mouse after administration of 200 mg kg^{-1} PhIP p.o., treated with *β*-glucuronidase and (ii) an equal portion of the same urine sample without treatment with *β*-glucuronidase.

Figure 3a1, a2 exemplify the presence and absence of two PhIP glucuronides without and with treatment of *β*-glucuronidase, respectively. *β*-glucuronidase and blank incubates were analyzed by LC–MS–MS as described in "Liquid Chromatography–Mass Spectrometry Detection". Treatment of urine with *β*-glucuronidase not only resulted in the disappearance of glucuronides but additionally showed a clear increase in the concentration of N2-OH-PhIP and 5-OH-PhIP (Fig. 3b1, b2).

Quantification of Metabolites

A strategic approach was developed to quantify metabolites of PhIP based on a certified reference standard of PhIP.

The use of a mass spectrometer for this purpose is not preferred as the increase in MS response per concentration unit is not expected to be equal for each metabolite. The preferred/predominant fragmentation site of each metabolite is dependent on the presence and position of terminal moieties. Metabolites of PhIP in which e.g. hydroxylation or sulfation has taken place, would predominantly fragment by loss of a hydroxyl or sulfate group, respectively, whereas the loss of the methyl moiety is predominant for PhIP. Each of these products fragment with a different yield, resulting in strongly varying fragmentation responses. Additionally, due to the large variation in polarity and elution times between metabolites, the ionization efficiency will also differ strongly. Therefore, quantification of PhIP metabolites based on the MS response of the parent PhIP molecule would not result in accurate results. UV detection rather than MS detection is in this case the preferred method.

The chromophore of PhIP is present in each metabolite. The maximum absorption wavelength changes minorly with the addition of hydroxyl groups and glucuronide moieties [30, 38, 39]. Quantification of PhIP metabolites based on a PhIP reference standard is therefore best performed by using UV absorption. Even though the UV absorption spectra of PhIP metabolites are very similar, we choose to analyze each metabolite at its specific maximum absorption wavelength, to ascertain accurate results, and assuming the molar extinction coefficient of PhIP metabolites to be similar to the molar extinction coefficient of PhIP [30]. Online absorption spectra were recorded and maximum absorption wavelengths defined. Typical spectra are presented in Fig. 4.

A solution of PhIP was diluted to three concentrations of 0.1, 1.0 and 10 μg mL^{-1}, respectively. These dilutions

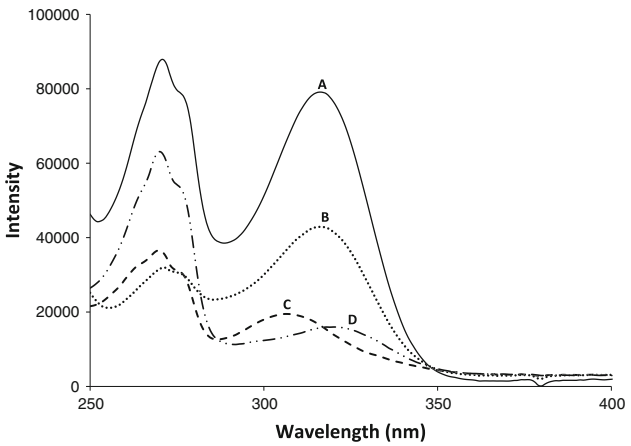

Fig. 4 Absorption spectrum of PhIP and three metabolites showing the influence of addition of a sulfate, glucuronide and hydroxyl group, respectively, on the maximum absorption wavelength. Spectra are measured online after injection of a diluted urine sample of a mouse treated with 200 mg kg^{-1} PhIP by oral gavage. **a** PhIP, **b** PhIP-4′-sulfate, **c** PhIP-N3-glucuronide, **d** 5-OH-PhIP

Table 4 Mass, retention time, maximum absorption wavelength and average concentration in mouse urine of PhIP and its metabolites

Analyte	Analyte number[a]	Parent mass $[M + H]^+$	Product mass $[M + H]^+$	t_r (min) LC–UV–MS[b]	t_r (min) LC–MS–MS[c]	λ_{max} (nm)	Average conc (ug mL^{-1}) $n = 5$	RSD (%) $n = 5$
PhIP	1	225	210	20.2	10.0	316	358	38.1
N2-OH-PhIP	2	241	223	17.7	11.1	318	38.6	24.7
5-OH-PhIP	3	241	223	13.3	9.9	316	26.8	16.3
N2-methyl-PhIP	4	239	224/223	27.8	10.4	306	6.51	13.3
PhIP-4′-sulfate	5	321	241	6.3	6.1	316	57.3	38.6
PhIP-5-sulfate	6	321	241	5.8	5.2	316	191	23.5
N2,4′-diOH-PhIP-sulfate	7	337	320/257	5.6	5.6	316	72.1	45.2
PhIP-N2-glucuronide	8	401	225	9.8	8.0	318	124	48.2
PhIP-N3-glucuronide	9	401	225	8.0	5.2	306	10.5	50.1
OH-PhIP-glucuronide_1	10	417	241	3.5	3.3	313	334	34.3
OH-PhIP-glucuronide_2	11	417	241	4.6	6.5	310	219	27.1
OH-PhIP-glucuronide_3	12	417	241/223	8.5	9.5	315	23.5	98.5
OH-PhIP-glucuronide_4	13	417	241/223	9.5	11.5	306	56.3	113

Average concentration and RSD is based on measurements in urine of five mice

[a] Numbering system is the same as in Fig. 1

[b] HPLC system as described in Table 2

[c] HPLC system as described in Table 3

Table 5 Inter-assay precision and stability parameters

Analyte	Analyte number[a]	Inter-assay precision (% CV) LC–UV[b]	Inter-assay precision (% CV) LC–MS–MS[c]	Stability (dev (%)) 2–8 °C, 22 h)
PhIP	1	10.6	5.72	4.29
N2-OH-PhIP	2	12.3	12.1	3.48
5-OH-PhIP	3	11.1	4.00	3.58
N2-methyl-PhIP	4	12.3	4.86	5.19
PhIP-4′-sulfate	5	14.4	3.85	8.98
PhIP-5-sulfate	6	14.9	3.53	9.41
N2,4′-diOH-PhIP-sulfate	7	13.4	8.86	10.3
PhIP-N2-glucuronide	8	13.8	7.53	4.61
PhIP-N3-glucuronide	9	11.4	7.56	3.04
OH-PhIP-glucuronide_1	10	11.2	5.67	6.61
OH-PhIP-glucuronide_2	11	11.9	10.4	−1.05
OH-PhIP-glucuronide_3	12	11.6	7.37	−7.88
OH-PhIP-glucuronide_4	13	11.8	12.1	7.47

dev deviation, *CV* coefficient of variation

[a] Numbering system is the same as in Fig. 1

[b] HPLC system as described in Table 2

[c] HPLC system as described in Table 3

were analyzed in triplicate using an LC–UV–MS set-up (UV set at 318 nm). Subsequently, a calibration curve (area versus nominal concentration) was fitted by least-squares linear regression using the reciprocal of the concentration ($1/x$) as a weighting factor. One urine sample was then analyzed in triplicate at three wavelengths i.e., 306, 318 and 340 nm. Depending on its λ_{max}, each metabolite was quantified by interpolation of its response, measured at either of the three wavelengths, on the calibration curve of PhIP. As the concentration calculations were based on the

molar extinction coefficient, the molecular mass of the metabolites was taken into account in the calculation. The urine sample in which PhIP and its metabolites were quantified based on the calibration curve of PhIP, was then designated to be a standard which was used to quantify PhIP and its metabolites in other urine samples. For that purpose, the standardized urine sample was subsequently analyzed on an LC–MS–MS set-up together with the remaining urine samples. The response of the metabolites in the remaining urine samples were quantified in triplicate based on the standardized urine sample which was also analyzed in triplicate in the same run. Results of these experiments are presented in Table 4.

Precision and Stability

Inter-assay precisions were within 15% for all analytes in both the LC–UV–MS and LC–MS–MS set-up.

The recovered concentration of PhIP and its metabolites was within 15% of the initial concentration when diluted urine was stored for 22 h at 2–8 °C in amber colored autosampler vials, providing enough time for the whole analysis as described above (Table 5). The lower limit of quantification of PhIP was determined to be approximately 1.0 ng mL^{-1}.

Conclusion

An assay was successfully developed for the quantification of PhIP and three of its phase I and nine of its phase II metabolites in mouse urine. This assay was based on liquid chromatography coupled to mass spectrometry and ultraviolet detection.

Metabolites were identified based on fragmentation patterns, relative retention times, UV absorption, degradation by β-glucuronidase, and NMR spectroscopy.

We provide a strategic way for quantification of analytes of which no reference standards are available. The presented assay will provide further insight into PhIP metabolism which is pivotal to understand its carcinogenic properties.

References

1. Sanz AM, Ayala JH, Gonzalez V, Afonso AM (2008) J Chromatogr B Anal Technol Biomed Life Sci 862:15–42
2. Shioya M, Wakabayashi K, Sato S, Nagao M, Sugimura T (1987) Mutat Res 191:133–138
3. Murkovic M (2004) J Chromatogr B Analy Technol Biomed Life Sci 802:3–10
4. Gooderham NJ, Creton S, Lauber SN, Zhu H (2007) Toxicol Lett 168:269–277
5. Esumi H, Ohgaki H, Kohzen E, Takayama S, Sugimura T (1989) Jpn J Cancer Res 80:1176–1178
6. Ito N, Hasegawa R, Imaida K, Tamano S, Hagiwara A, Hirose M, Shirai T (1997) Mutat Res 376:107–114
7. Shirai T, Sano M, Tamano S, Takahashi S, Hirose M, Futakuchi M, Hasegawa R, Imaida K, Matsumoto K, Wakabayashi K, Sugimura T, Ito N (1997) Cancer Res 57:195–198
8. Zheng W, Gustafson DR, Sinha R, Cerhan JR, Moore D, Hong CP, Anderson KE, Kushi LH, Sellers TA, Folsom AR (1998) J Natl Cancer Inst 90:1724–1729
9. Reistad R, Frandsen H, Grivas S, Alexander J (1994) Carcinogenesis 15:2547–2552
10. Frandsen H (2007) Food Chem Toxicol 45:863–870
11. Gooderham NJ, Murray S, Lynch AM, Yadollahi-Farsani M, Zhao K, Boobis AR, Davies DS (2001) Drug Metab Dispos 29:529–534
12. Chen C, Ma X, Malfatti MA, Krausz KW, Kimura S, Felton JS, Idle JR, Gonzalez FJ (2007) Chem Res Toxicol 20:531–542
13. Crofts FG, Sutter TR, Strickland PT (1998) Carcinogenesis 19:1969–1973
14. Cheung C, Ma X, Krausz KW, Kimura S, Feigenbaum L, Dalton TP, Nebert DW, Idle JR, Gonzalez FJ (2005) Chem Res Toxicol 18:1471–1478
15. Suzuki H, Morris JS, Li Y, Doll MA, Hein DW, Liu J, Jiao L, Hassan MM, Day RS, Bondy ML, Abbruzzese JL, Li D (2008) Carcinogenesis 29:1184–1191
16. Minchin RF, Reeves PT, Teitel CH, McManus ME, Mojarrabi B, Ilett KF, Kadlubar FF (1992) Biochem Biophys Res Commun 185:839–844
17. Malfatti MA, Buonarati MH, Turteltaub KW, Shen NH, Felton JS (1994) Chem Res Toxicol 7:139–147
18. Chou HC, Lang NP, Kadlubar FF (1995) Cancer Res 55:525–529
19. Glatt H (1997) FASEB J. 11:314–321
20. Glatt H (2000) Chem Biol Interact 129:141–170
21. Jamin EL, Arquier D, Canlet C, Rathahao E, Tulliez J, Debrauwer L (2007) J Am Soc Mass Spectr 18:2107–2118
22. Wild D, Dirr A (1989) Mutagenesis 4:446–452
23. Lin D, Kaderlik KR, Turesky RJ, Miller DW, Lay JO Jr, Kadlubar FF (1992) Chem Res Toxicol 5:691–697
24. Frandsen H (2008) Food Chem Toxicol 46:3200–3205
25. Frandsen H, Frederiksen H, Alexander J (2002) Food Chem Toxicol 40:1125–1130
26. Frandsen H, Alexander J (2000) Carcinogenesis 21:1197–1203
27. Kulp KS, Knize MG, Malfatti MA, Salmon CP, Felton JS (2000) Carcinogenesis 21:2065–2072
28. Kaderlik KR, Minchin RF, Mulder GJ, Ilett KF, Daugaard-Jenson M, Teitel CH, Kadlubar FF (1994) Carcinogenesis 15:1703–1709
29. Buonarati MH, Turteltaub KW, Shen NH, Felton JS (1990) Mutat Res 245:185–190
30. Fede JM, Thakur AP, Gooderham NJ, Turesky RJ (2009) Chem Res Toxicol 22:1096–1105
31. Langouet S, Paehler A, Welti DH, Kerriguy N, Guillouzo A, Turesky RJ (2002) Carcinogenesis 23:115–122
32. Teunissen SF, Rosing H, Schinkel AH, Schellens JH (2010) J Chromatogr B Analy Technol Biomed Life Sci 878:3199
33. Teunissen SF, Vlaming ML, Rosing H, Schellens JH, Schinkel AH, Beijnen JH (2010) J Chromatogr B Analy Technol Biomed Life Sci 878:2353–2362
34. Kulp KS, Knize MG, Fowler ND, Salmon CP, Felton JS (2004) J Chromatogr B Analy Technol Biomed Life Sci 802:143–153
35. Knize MG, Kulp KS, Malfatti MA, Salmon CP, Felton JS (2001) J Chromatogr A 914:95–103
36. Jerschow A, Müller N (1997) Suppression of convection artifacts in stimulated-echo diffusion experiments. Double-stimulated-echo experiments. J Magn Reson 125:372

37. Stejskal EO, Tanner JE (1965) Spin diffusion measurements: spin echoes in the presence of a time-dependent field gradient. J Chem Phys 42:288
38. Crofts FG, Strickland PT, Hayes CL, Sutter TR (1997) Carcinogenesis 18:1793–1798
39. Styczynski PB, Blackmon RC, Groopman JD, Kensler TW (1993) Chem Res Toxicol 6:846–851
40. Malfatti MA, Felton JS (2001) Carcinogenesis 22:1087–1093